Study of A PMSM Model Incorporating Structural and Saturation Saliencies

Ying Yan[1], Jianguo Zhu[1], Haiwei Lu[1], Youguang Guo[1] and Shuhong Wang[2]
[1]Faculty of Engineering, University of Technology, Sydney, PO Box 123, Broadway, NSW 2007, Australia
[2]Faculty of Electrical Engineering, Xi'an Jiaotong University, Xi'an, 710049, China

***Abstract*—Sensorless permanent magnet synchronous motor (PMSM) drive systems have become very attractive due to their advantages, such as reduction of hardware complexity and hence the system cost and increment of system reliability. In order to correctly obtain the rotor position information required for the appropriate control, various methods have been proposed. Among them, the most versatile method makes use of the structural and magnetic saturation saliencies of the PMSM. This paper presents a non-linear model of PMSMs considering the saliencies. The phase inductances of a PMSM are measured and expressed in Fourier series versus stator winding currents and rotor positions according to the inductance pattern. The simulated dynamic performance is compared with that based on a model without considering saliency to verify the effectiveness of the proposed PMSM model.**

Keywords-PMSM model, structural saliency, saturation saliency, inductance.

I. INTRODUCTION

Sensorless control of permanent magnet synchronous motors (PMSMs) has become very attractive because of its several advantages over the systems with mechanical position sensors, such as significant reduction of hardware complexity and hence the cost and increment of the system reliability. A great amount of research has been conducted on position sensorless techniques and various methods have been proposed. Among them, the most versatile method identifies the rotor position by detecting the structural and magnetic saturation saliencies, which exist even in surface mounted PMSMs [1-2].

The structural saliency is caused by the mechanical structure of the machine and is seldom affected by the stator current. For the electric machines with large structural saliency, e.g. interior mounted PMSM, the structural saliency-based rotor position identification can be very effective.

The magnetic saliency is caused by the saturation of magnetic core. In a PMSM, this kind of saliency is mainly caused by the permanent magnets (PMs) on the rotor, and it is usually not significant compared to the structural saliency. In addition, it is affected by the magnetic field produced by the stator current. It becomes a challenge to detect the rotor position of a PMSM with little structural saliency, such as a surface mounted PMSM.

In this paper, a non-linear PMSM model which incorporates both the structural and saturation saliencies is derived in order to verify effectively the existing and new position detection methods. In the model, the saliencies of the motor are reflected by the variation of the stator winding inductances with respect to the rotor position. In order to obtain the relationship between the inductance and rotor position, an inductance model is established based on the Fourier series and is applied on a surface mounted PMSM. Dynamic simulation using the derived model is carried out and the results are compared with the ones without considering the saliencies.

II. NON-LINEAR MODEL OF A PMSM WITH SALIENCIES

Fig. 1 illustrates schematically the structure and flux linkage of a surface mounted PMSM (SPMSM). When the motor saliencies are taken into account, the conventional model of PMSM is inaccurate since the inductances of the motor will be the functions of the rotor position due to the saliencies. Therefore, an improved PMSM model is required.

A. Flux Linkage and Circuit Equations

In a PMSM, the rotor field is the dominant field which determines the operating point of the magnetic core. Although the characteristics of the magnetic core is non-linear, the magnetic circuit can be considered as piecewisely linearized around the operating point *P* at a given rotor position, as shown in Fig. 2. Thus, as an example, the total flux linkage of phase *a*,

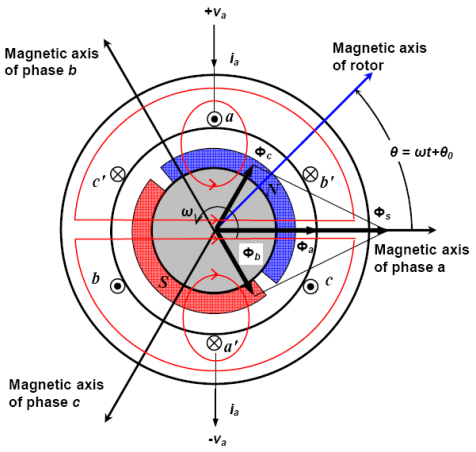

Figure 1. Structure and flux linkage of an SPMSM

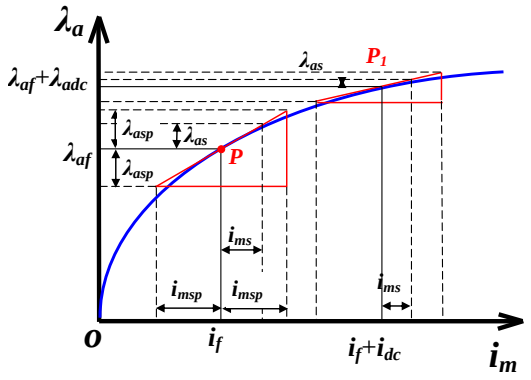

Figure 2. Linerazation of the magnetic circuit in an SPMSM for a given rotor position

λ_a, can be separated into two components,

$$\lambda_a = \lambda_{as}(i_{ms}, \theta) + \lambda_{af}(\theta) \tag{1}$$

where λ_{af} is the flux linkage component of phase *a* produced by the PMs, λ_{as} the flux linkage component of phase *a* corresponding to the resultant stator magnetization current i_{ms}, and the subscript *p* indicates the peak value. The flux linkage λ_{as} can be further separated into components attributed by individual stator phase currents. Consequently, the total flux linkage of phase *a* can be expressed as:

$$\lambda_a = \lambda_{aa} + \lambda_{ab} + \lambda_{ac} + \lambda_{af} \tag{2}$$

where λ_{aa}, λ_{ab}, and λ_{ac} are the flux linkage components of phase *a* corresponding to each phase current. Under the assumption of linearization, the flux linkage components, λ_{aa}, λ_{ab}, and λ_{ac} can be considered proportional to the corresponding currents:

$$\lambda_{aa} = L_{aa}(i_a, \theta) i_a,\ \lambda_{ab} = L_{ab}(i_b, \theta) i_b, \text{ and } \lambda_{ac} = L_{ac}(i_c, \theta) i_c$$

The proportionality coefficients L_{aa}, L_{ab}, and L_{ac}, which are determined by the gradient of the magnetization curve at the operating point, are defined as the self and mutual inductances of the phase windings. The flux linkages of phase *b* and *c* can be obtained similarly.

The electric circuit equations of the three-phase stator windings can be written as,

$$v_s = R_s i_s + \frac{d\lambda_s}{dt},\ s = a, b, c \tag{3}$$

where v_s, i_s, and R_s are the phase voltages, currents, and winding resistances, respectively. Based on the previous derivation, the following differential equations can be obtained:

$$\begin{bmatrix} v_a \\ v_b \\ v_c \end{bmatrix} = \begin{bmatrix} R_a & 0 & 0 \\ 0 & R_b & 0 \\ 0 & 0 & R_c \end{bmatrix} \begin{bmatrix} i_a \\ i_b \\ i_c \end{bmatrix} + [L_T] \begin{bmatrix} \frac{di_a}{dt} \\ \frac{di_b}{dt} \\ \frac{di_c}{dt} \end{bmatrix} + \begin{bmatrix} e_{af} + e_{a\theta} \\ e_{bf} + e_{b\theta} \\ e_{cf} + e_{c\theta} \end{bmatrix} \tag{4}$$

where

$$[L_T] = \begin{bmatrix} L_{aa} + i_a \frac{\partial L_{aa}}{\partial i_a} & L_{ab} + i_b \frac{\partial L_{ab}}{\partial i_b} & L_{ac} + i_c \frac{\partial L_{ac}}{\partial i_c} \\ L_{ab} + i_a \frac{\partial L_{ab}}{\partial i_a} & L_{bb} + i_b \frac{\partial L_{bb}}{\partial i_b} & L_{bc} + i_c \frac{\partial L_{bc}}{\partial i_c} \\ L_{ac} + i_a \frac{\partial L_{ac}}{\partial i_a} & L_{bc} + i_b \frac{\partial L_{bc}}{\partial i_b} & L_{cc} + i_c \frac{\partial L_{cc}}{\partial i_c} \end{bmatrix} \tag{5}$$

and $e_{af} = \omega_r d\lambda_{af}/d\theta$, $e_{bf} = \omega_r d\lambda_{bf}/d\theta$, and $e_{cf} = \omega_r d\lambda_{cf}/d\theta$ are the electromotive forces (*emfs*) induced by the PMs. In addition,

$$e_{a\theta} = \omega_r \left(i_a \frac{dL_{aa}}{d\theta} + i_b \frac{dL_{ab}}{d\theta} + i_c \frac{dL_{ac}}{d\theta} \right) \tag{6}$$

$$e_{b\theta} = \omega_r \left(i_a \frac{dL_{ab}}{d\theta} + i_b \frac{dL_{bb}}{d\theta} + i_c \frac{dL_{bc}}{d\theta} \right) \tag{7}$$

and

$$e_{c\theta} = \omega_r \left(i_a \frac{dL_{ac}}{d\theta} + i_b \frac{dL_{bc}}{d\theta} + i_c \frac{dL_{cc}}{d\theta} \right) \tag{8}$$

are the *emfs* induced by the variation of flux linkage due to the saliencies, where $\omega_r = d\theta/dt$ is the mechanical angular speed of the rotor.

B. *Electromagnetic Torque*

The electromagnetic torque of the PMSM can be obtained by the derivative of the system co-energy with respect to the rotor angle, i.e. $T = \partial W_f'/\partial\theta$. The electromagnetic torque can be found by:

$$T = \frac{\partial \lambda_{af}}{\partial \theta} i_a + \frac{\partial \lambda_{bf}}{\partial \theta} i_b + \frac{\partial \lambda_{cf}}{\partial \theta} i_c + \frac{\partial L_{aa}}{\partial \theta} \frac{i_a^2}{2} + \frac{\partial L_{bb}}{\partial \theta} \frac{i_b^2}{2} + \frac{\partial L_{cc}}{\partial \theta} \frac{i_c^2}{2} + \frac{2\partial L_{ab}}{\partial \theta} i_a i_b + \frac{2\partial L_{ac}}{\partial \theta} i_a i_c + \frac{2\partial L_{bc}}{\partial \theta} i_b i_c \tag{9}$$

From (9), it can be concluded that there are two kinds of electromagnetic torque. One is the torque produced by the PMs, which is determined by rotor flux linkage, and the other is the torque due to the saliencies, which is caused by the variation of the phase inductances.

III. NON-LINEAR INDUCTANCE PATTERN

A. *Non-linear Inductance Pattern*

Accurate prediction of the motor dynamic performance requires a motor model with accurate parameters, especially the phase inductances. As discussed above, the structural and magnetic saturation saliencies can be reflected by the variation of the self- and mutual inductances of the stator windings.

According to the motor structure, the phase inductance is a periodic function of angular rotor position. Therefore, the

relationship between the phase inductance and the rotor position can be expressed by a Fourier series:

$$L(\theta) = a_0 + \sum_{m=1}^{n} \left(a_m \cos m\theta + b_m \sin m\theta \right) \tag{10}$$

The number of terms of the Fourier series is determined through the best curve fitting result from the experimental phase inductances [3]. In addition, due to the non-linear characteristics of the magnetic core, the inductances vary with the stator current. Consequently, different sets of coefficient a_0, a_m, and b_m ($m=1, 2, \ldots, n$) can be obtained at different currents, and expressed by the functions of corresponding current. Therefore, the inductance can be further expressed as:

$$L(i,\theta) = a_0(i) + \sum_{m=1}^{n} \left(a_m(i) \cos m\theta + b_m(i) \sin m\theta \right) \tag{11}$$

For a group of known values of phase inductance, $L(\theta_j, i_k)$, the inductance pattern can be worked out by the method of non-linear curve fitting, where j and k refer to the various experimental rotor positions and currents, respectively.

The nonlinear model of the self- and mutual- inductances can readily be incorporated into the PMSM model presented in Section II by simply substituting the following relationships into the model:

$$\frac{dL(\theta, i_k)}{d\theta} = \sum_{m=1}^{n} \left((-m) a_m(i_k) \sin m\theta + m b_m(i_k) \cos m\theta \right) \tag{12}$$

$$\frac{dL(\theta_j, i)}{di} = \frac{da_0(i)}{di} + \sum_{m=1}^{n} \left(\frac{da_m(i)}{di} \cos m\theta_j + \frac{db_m(i)}{di} \sin m\theta_j \right) \tag{13}$$

B. Experimental Phase Inductances

In order to acquire the correct inductances of the motor, some aspects should be considered in advance. When a PMSM is in its normal operating state, the total flux is composed of both the stator and rotor fluxes, ($\psi_t = \psi_r + \psi_s$), and the influence of the stator flux ψ_s cannot be neglected. Due to the stator flux, the magnetic core becomes more saturated at some positions and less saturated at other positions. Therefore, the phase inductance pattern will be affected by the stator flux.

In order to estimate the saturation effect at various stator fluxes, several DC offsets, i_{dc}, are used to emulate the effect of the three-phase currents. Based on the analysis of the relationship between the saturation of magnetic core and the inductance variation, a method for measuring the phase inductances is designed and the saturation effect due to stator currents can be reflected in the inductance patterns measured by this method.

The measurement system is shown in Fig. 3. The experiment is carried out on a 6-pole SPMSM. The rotor of the motor is locked by a dividing head. Various DC offsets are injected to one of the stator windings. Meanwhile, a small AC current is applied to one phase while the other two are open-circuited. The voltage, current and power of the excited phase are measured and the open-circuit voltages of the other two phases are also recorded. The self- and mutual inductances of phases *a*, *b* and *c* at different rotor positions and stator fluxes can then be calculated via circuit analysis**.** The self-inductances of phase *a*, L_{ssa}, at various rotor positions with and without DC offsets are illustrated in Fig. 4.

According to the magnetic flux distribution in a PMSM, it can be concluded that the inductances by considering structural and saturation saliencies are the functions of amplitudes and angles of both stator and rotor fluxes, $L(\theta_s, \theta_r, |\psi_s|, |\psi_r|)$, where θ_s is the position of the stator flux, θ_r the position of rotor flux, and $|\psi_s|$ and $|\psi_r|$ are the amplitudes of the stator and rotor fluxes. The amplitude of the rotor flux can be considered as constant, while the amplitudes of the stator flux at a given i_{dc} is also constant. Under this condition, the inductances with the incorporation of structural and saturation saliencies could be simply expressed as a function of various θ_s and θ_r.

Moreover, if the machine is assumed ideally symmetric and the inductances of the three phases are identical, it can be known that the inductance patterns of phases *a*, *b* and *c* are of the same shape with ±120º phase shift due to the symmetrical distribution of three phase stator windings.

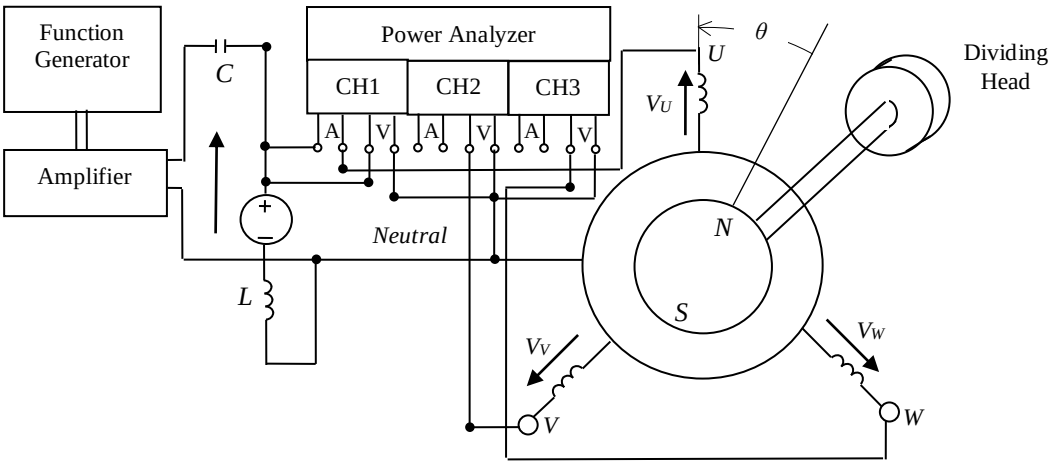

Figure 3. Setup of the testing system

In order to make the estimation of the inductance patterns easier, the angles between the stator flux, ψ_s, and stator winding axes of phases *a*, *b* and *c*, which are defined as α_a, α_b and α_c, and the angle between the stator flux and rotor fluxes, δ, as shown in Figs. 5-7, are used in the inductance model instead of θ_s, θ_r. For arbitrary α_a, α_b, α_c, and δ, the phase inductances can be expressed as $L_{saa}(\alpha_a, \delta)$, $L_{sbb}(\alpha_b, \delta)$ and $L_{scc}(\alpha_c, \delta)$, respectively. Due to the symmetrical distribution of the three phase windings, at $\alpha_a=\alpha_b=\alpha_c=\alpha$ and a given δ, it is known that $L_{saa}(\alpha, \delta) = L_{sbb}(\alpha, \delta) = L_{scc}(\alpha, \delta)$, where α is the angle between the stator flux and axis of phase *a* stator winding.

Based on the measured self- and mutual inductances of phases *a*, *b* and *c* with DC offsets injected to phase *a*, the self inductance patterns, $L_{ss}(\alpha, \theta_r, i_s)$, at a given α can be estimated as the following by (11):

$$L_{ss}(\alpha,\theta_r,i_s) = a_0(i_s) + \sum_{n=1}^{8}\left(a_n(i_s)\cos(n\theta_r) + b_n(i_s)\sin(n\theta_r)\right) \tag{14}$$

By the symmetrical analysis shown in Figs. 5-7, the inductances at the following positions are therefore obtained: 1) $\alpha=0^o$ and $\delta=0^o$-360^o; 2) $\alpha=120^o$ and $\delta=0^o$-360^o; 3) $\alpha=240^o$ and $\delta=0^o$-360^o. The phase *a* inductance patterns at various stator and rotor fluxes can be estimated by linear interpolation of the known inductance patterns at these positions and various amplitudes of equivalent stator fluxes determined by different values of DC offsets. The inductance patterns at each degree of α and θ_r and each ampere of the stator current, i_s, $L_{ssa}(\alpha=0^o$-360^o, $\theta_r=0^o$-360^o, $\lfloor i_s \rfloor)$, could be expressed in a matrix of $(N\times M\times K)$ at various α, θ_r, and i_s:

$$L_{ssai} = \begin{bmatrix} L_{ss}(\alpha_1,\theta_{r1},i_{si}) & L_{ss}(\alpha_2,\theta_{r1},i_{si}) & \cdots & L_{ss}(\alpha_N,\theta_{r1},i_{si}) \\ L_{ss}(\alpha_1,\theta_{r2},i_{si}) & L_{ss}(\alpha_2,\theta_{r2},i_{si}) & \cdots & L_{ss}(\alpha_N,\theta_{r2},i_{si}) \\ L_{ss}(\alpha_1,\theta_{r3},i_{si}) & L_{ss}(\alpha_2,\theta_{r3},i_{si}) & \cdots & L_{ss}(\alpha_N,\theta_{r2},i_{si}) \\ \vdots & \vdots & \cdots & \vdots \\ L_{ss}(\alpha_1,\theta_{rM},i_{si}) & L_{ss}(\alpha_2,\theta_{rM},i_{si}) & \cdots & L_{ss}(\alpha_N,\theta_{rM},i_{si}) \end{bmatrix} \tag{15}$$

where the subscript $i=1,2,3,\ldots, K$.

The inductance patterns of phases *b* and *c* can be obtained by shifting the rotor position in (15) with ±120º, respectively:

$$L_{ssb} = L_{ssa}\left(\alpha,\left(\theta_r - 120^\circ\right),i_s\right) \tag{16}$$

$$L_{ssc} = L_{ssa}\left(\alpha,\left(\theta_r + 120^\circ\right),i_s\right) \tag{17}$$

Similar procedure can be applied for the estimation of mutual inductance. The results can be used in (5) for the motor performance analysis.

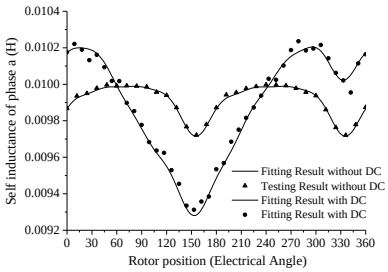

Figure 4. Measured self-inductances and fitting curves

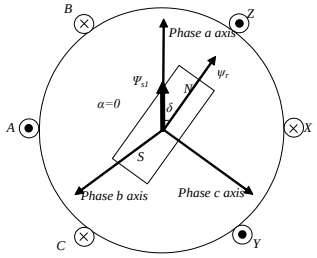

Figure 5. Rotor and stator flux linked with phase *a* with DC offset to phase *a*

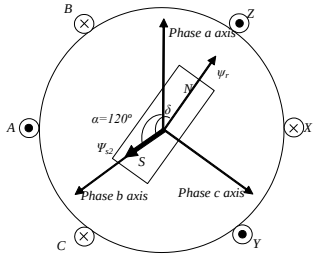

Figure 6. Rotor and stator flux linked with phase *b* with DC offset to phase *a*

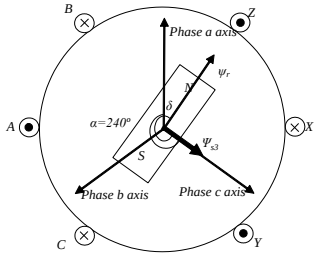

Figure 7. Rotor and stator flux linked with phase *c* with DC offset to phase *a*

IV. Dynamic Simulation of PMSM Model

Based on the proposed model and experimental parameter identification, dynamic simulation of the PMSM using this model incorporating the structural and saturation saliencies is conducted. The simulation based on the model without considering saliencies is also conducted for comparison.

A. Simulation Results of the Model by Considering Saliencies

Based on the PMSM model by considering saliencies and the measured parameters, simulation is firstly conducted to estimate the dynamic performance of the motor. The input voltage is a balanced three phase sinusoidal waveform with amplitude value of 12 V and frequency of 5 Hz.

The stator currents of the motor are shown in Fig. 8. The total back *emf*, and the back *emf* caused by structural saliency are illustrated in Figs. 9-10. The total electromagnetic torque

and the electromagnetic torque caused by saliencies with a load of 0.5 Nm are shown in Fig. 11.

B. Simulation Results of the Model without Considering Saliencies

With the previously measured PMSM parameters, the dynamic simulation for a conventional model without considering saliencies is performed and a Matlab program is complied by using Euler method for the numerical calculation. In order to compare with the previous results, the same initial and load conditions are set in the simulation. The electromagnetic torque and rotor speed are compared with those based on the proposed model with saliency, as shown in Figs. 12 and 13.

It can be seen from Figs. 12 and 13 that there is very small difference of the electromagnetic torque and rotor position obtained by the two models and this is mainly due to the surface-mounted permanent magnet rotor structure. For this specific motor, the saliency effect is not so apparent as motors with large saliencies, such as interior type PMSM or switch reluctance motor. However, the proposed model is capable of analyzing various types of motor by considering saliencies. Moreover, the inclusion of the structural and saturation saliencies provides a possibility to estimate the N-S poles of the PM on the rotor, so that the estimation of rotor position in sensorless control schemes could be numerically simulated based on the model. In addition, more accurate torque calculation could be useful for the dynamic state estimation in the torque control scheme, such as the direct torque control scheme.

V. CONCLUSIONS

A non-linear PMSM model incorporating both the structural and magnetic saturation saliencies was derived in this paper. In the equivalent electric circuit, the saliencies are reflected by the variation of the stator winding inductances with respect to the rotor positions and stator currents. The nonlinear inductances at various rotor positions and stator currents are discussed and experimentally obtained from a surface mounted PMSM. Fourier series analysis is employed to describe the relation of the inductance and rotor position. Dynamic simulation considering the saliencies is performed based on the parameters obtained from the testing motor. The results are compared with that from a model without considering saliency. The saliency in the studied SPMSM is mainly due to the magnetic saturation and could be used to estimate the angle between rotor flux and stator flux. The incorporation of the structural and saturation saliencies provides a possibility to estimate the N-S poles of the PM on the rotor, so that the estimation of rotor position in sensorless control schemes could be numerically simulated based on the model. The proposed model is capable of analyzing various types of motor by considering saliencies.

REFERENCES

[1] P.L. Jansen and R.D. Lorenz, "Transducerless position and velocity estimation in induction and salient AC machines," in *Record of IEEE IAS Annual Meeting*, Oct. 1994, vol. 1, pp. 488-495.

[2] L. Wang and R.D. Lorenz, "Rotor position estimation for permanent magnet synchronous motor using saliency-tracking self-sensing method," in *Record of IEEE IAS Annual Meeting*, Oct. 2000, vol. 1, pp. 445-450.

[3] P. Cui, J.G. Zhu, Q.P. Ha, G.P. Hunter, and V.S. Ramsden, "Simulation of non-linear switched reluctance motor drive with PSIM," in *Proc. 5th Int. Conf. on Electrical Machines and Systems*, Aug. 2001, vol. 1, pp. 1061-1064.

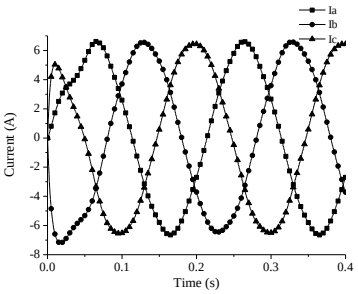

Figure 8. Phase current by the model with structural saliency

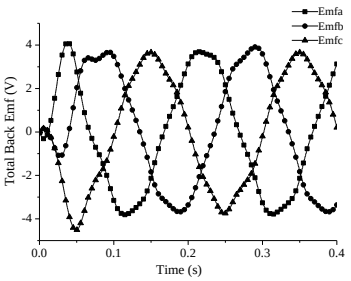

Figure 9. Total back *emf* by the model with structural saliency

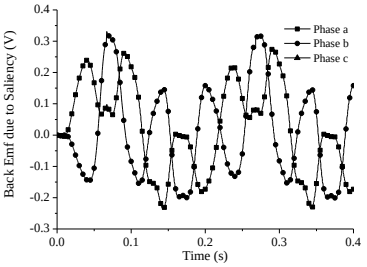

Figure 10. The back *emf* due to structural saliency

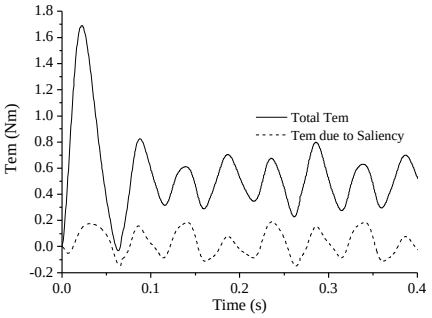

Figure 11. Total electromagnetic torque and electromagnetic torque caused by saliency, with a load of 0.5 Nm

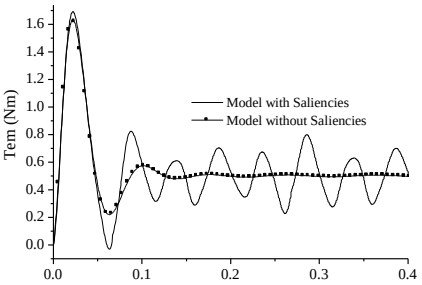

Figure 12. Comparison of the electromagnetic torque by two models

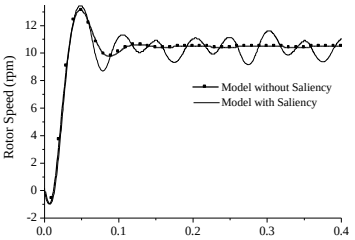

Figure 13. Comparison of the rotor speed by two models